

Mechanism reduction for multicomponent surrogates: a case study using toluene reference fuels

Kyle E. Niemeyer and Chih-Jen Sung

Supplementary material

The skeletal mechanisms generated in this work will be included as supplemental materials upon publication, and the MARS reduction package may be obtained upon request to the authors. The following figures are those omitted from the main text for brevity.

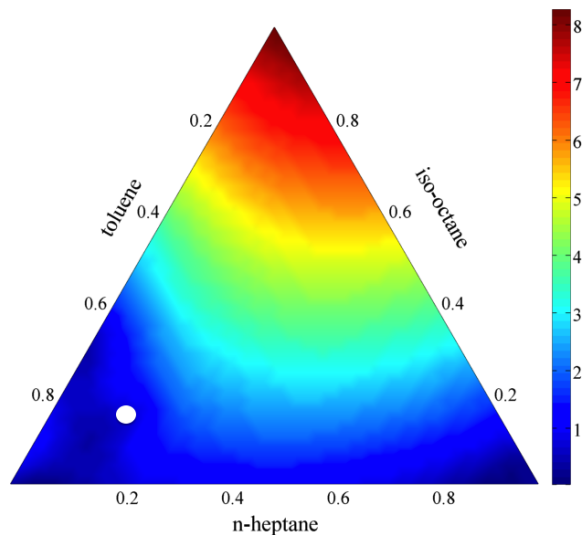
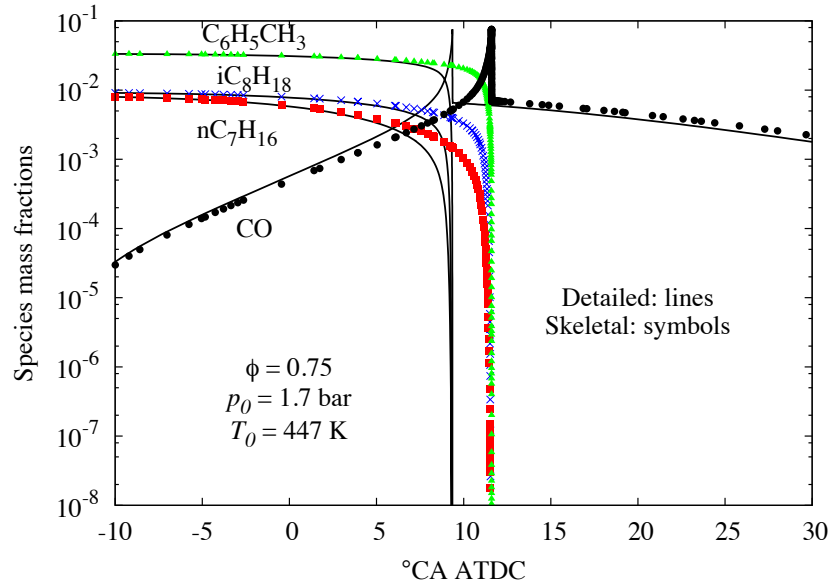
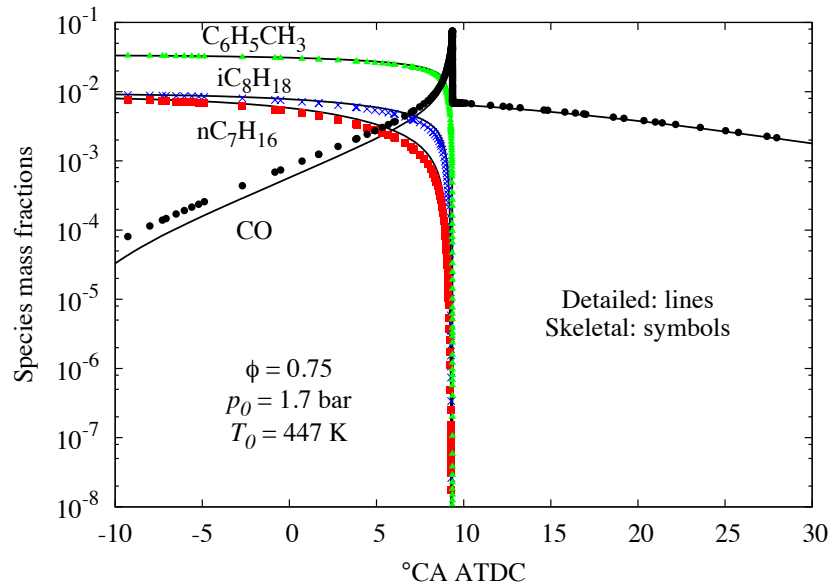


Figure S1: Percent error in predicted ignition delay for constant volume autoignition using the 30%-error high-temperature skeletal mechanism (173 species and 689 reactions) with a varying fuel composition, using initial conditions of 1,200 K, 10 atm, and $\phi = 1.0$. The white circle indicates the TRF1 mixture composition used for the reduction procedure.

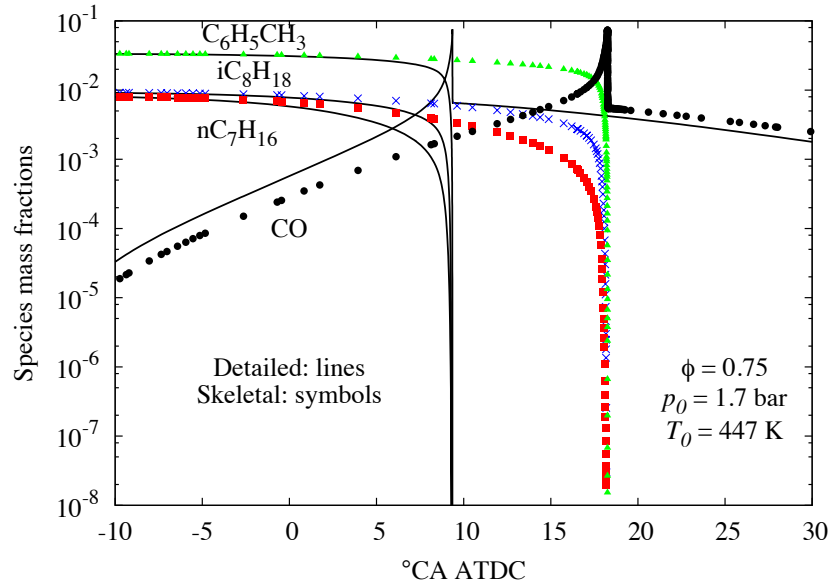


(a) Original CA

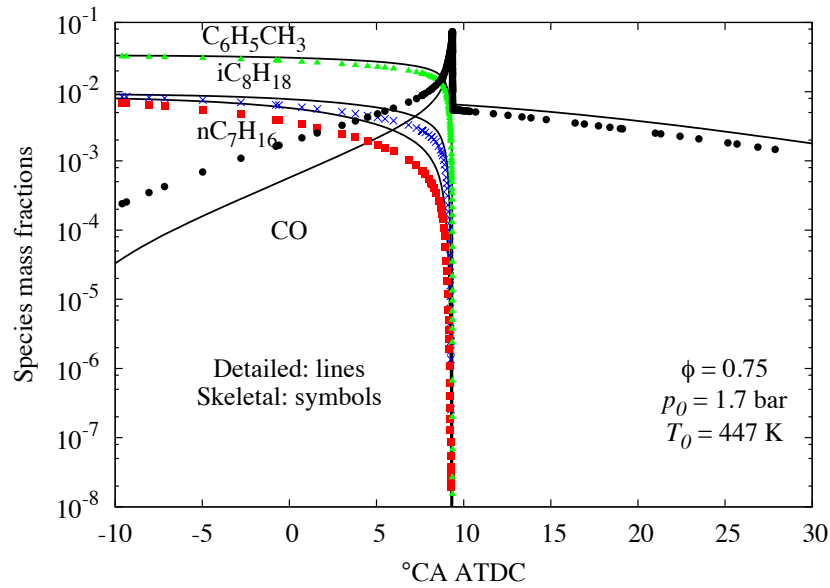


(b) Shifted CA

Figure S2: Comparison of major species mass fractions between the detailed TRF and 10%-error comprehensive skeletal (386 species and 1,591 reactions) mechanisms for a single-zone HCCI simulation with the IC1 initial conditions specified in Table 1. The shifted CA plot is based on ignition delay timing.

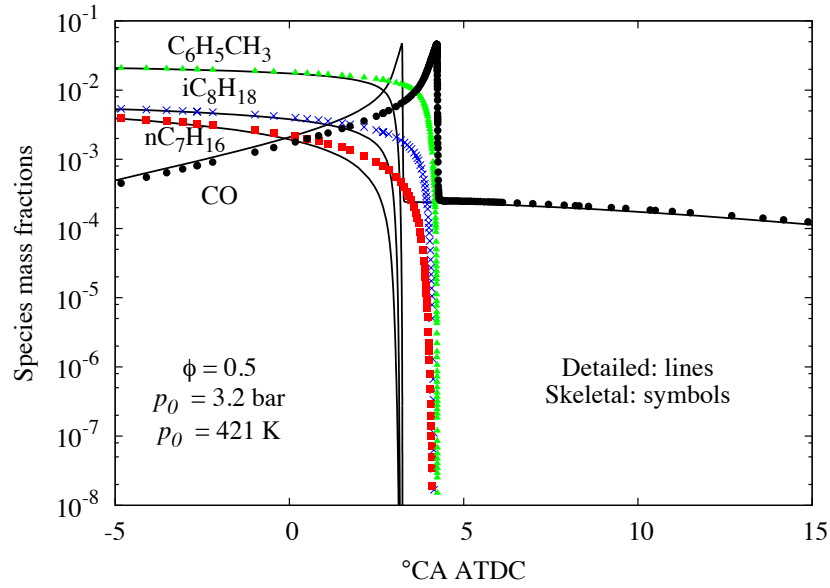


(a) Original CA

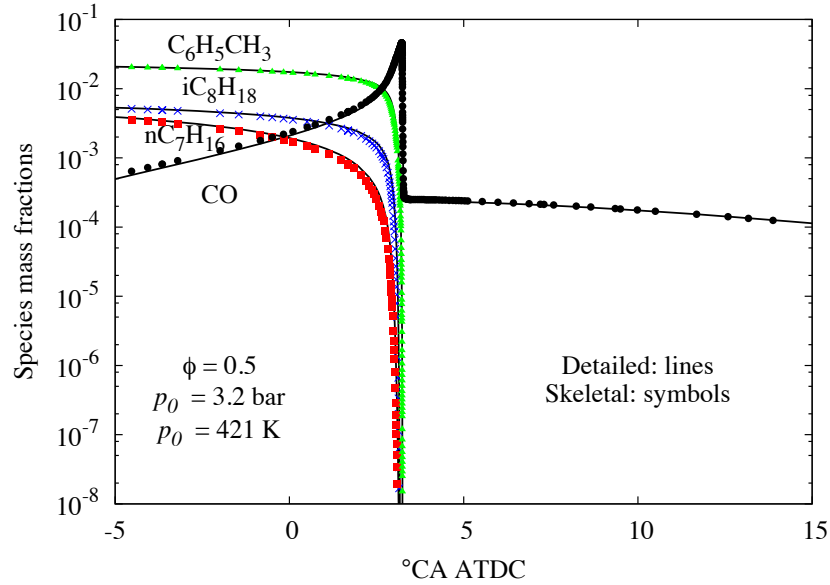


(b) Shifted CA

Figure S3: Comparison of major species mass fractions between the detailed TRF and 30%-error comprehensive skeletal (276 species and 936 reactions) mechanisms for a single-zone HCCI simulation with the IC1 initial conditions specified in Table 1. The shifted CA plot is based on ignition delay timing.

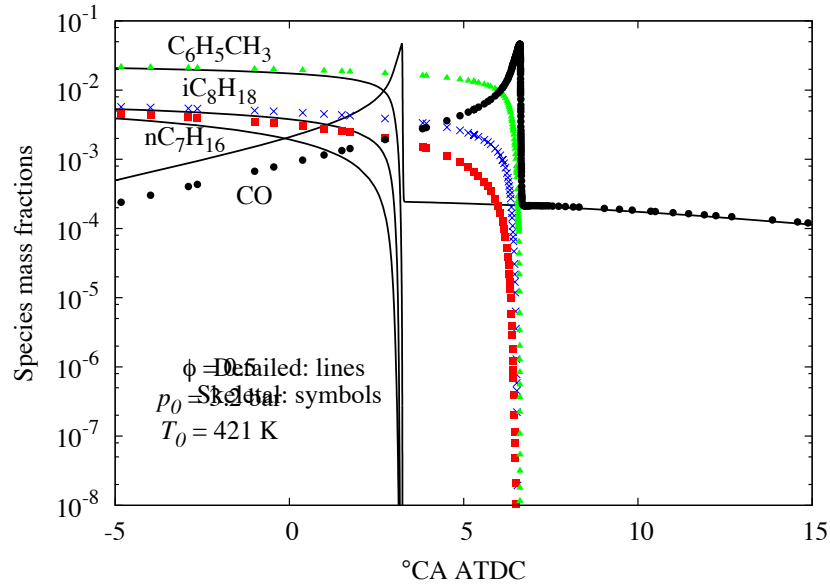


(a) Original CA

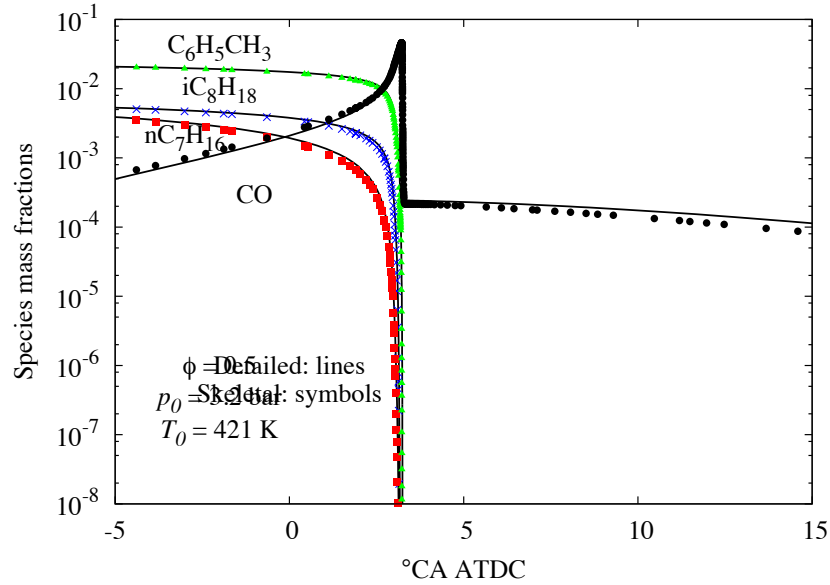


(b) Shifted CA

Figure S4: Comparison of major species mass fractions between the detailed TRF and 10%-error comprehensive skeletal (386 species and 1,591 reactions) mechanisms for a single-zone HCCI simulation with the IC2 initial conditions specified in Table 1. The shifted CA plot is based on ignition delay timing.

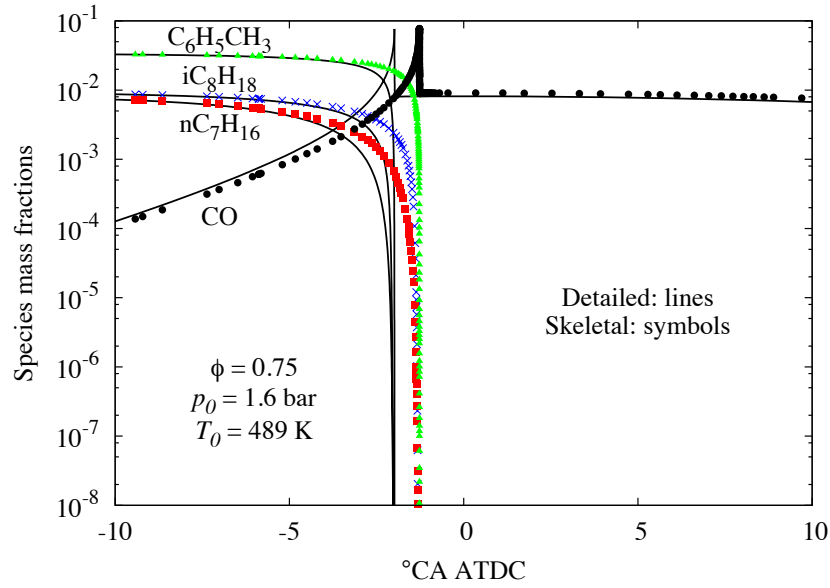


(a) Original CA

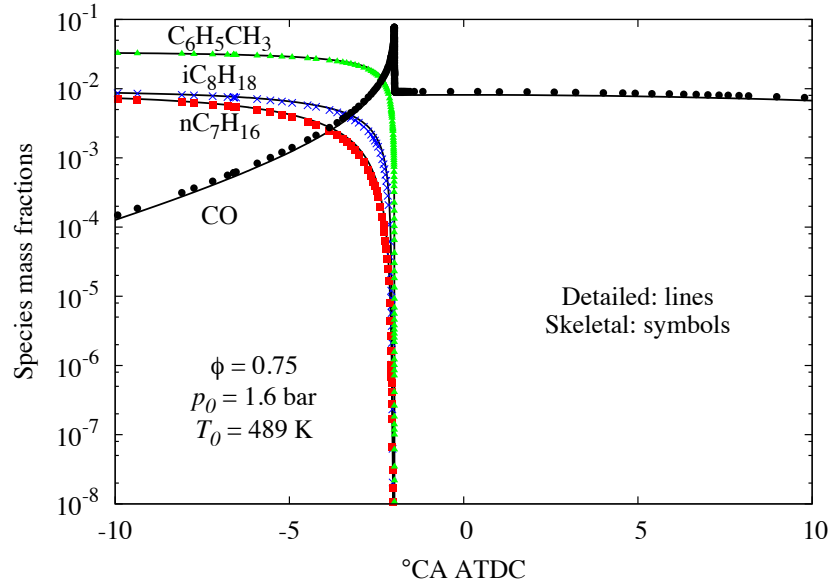


(b) Shifted CA

Figure S5: Comparison of major species mass fractions between the detailed TRF and 30%-error comprehensive skeletal (276 species and 936 reactions) mechanisms for a single-zone HCCI simulation with the IC2 initial conditions specified in Table 1. The shifted CA plot is based on ignition delay timing.

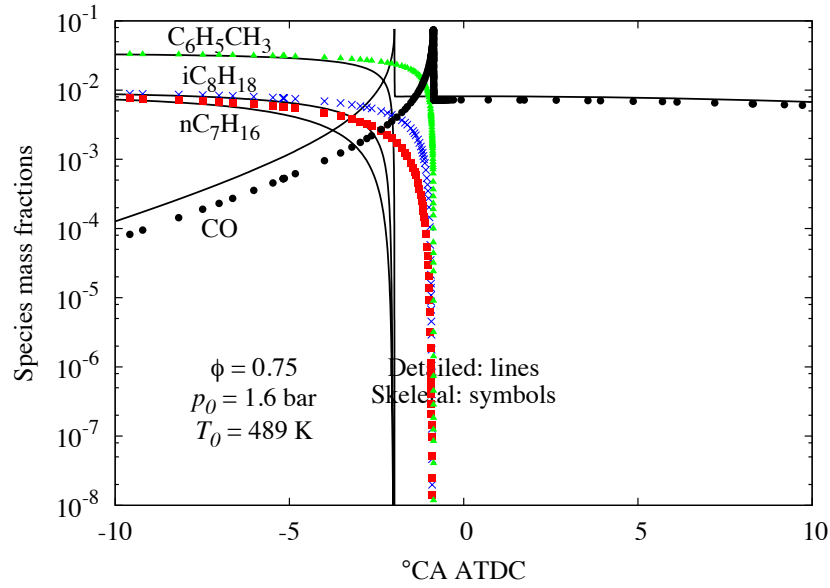


(a) Original CA

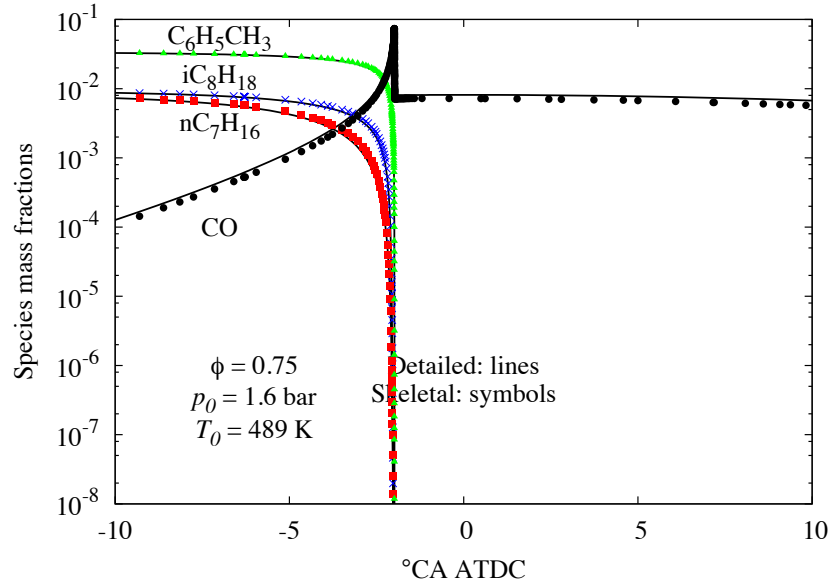


(b) Shifted CA

Figure S6: Comparison of major species mass fractions between the detailed TRF and 10%-error comprehensive skeletal (386 species and 1,591 reactions) mechanisms for a single-zone HCCI simulation with the IC3 initial conditions specified in Table 1. The shifted CA plot is based on ignition delay timing.

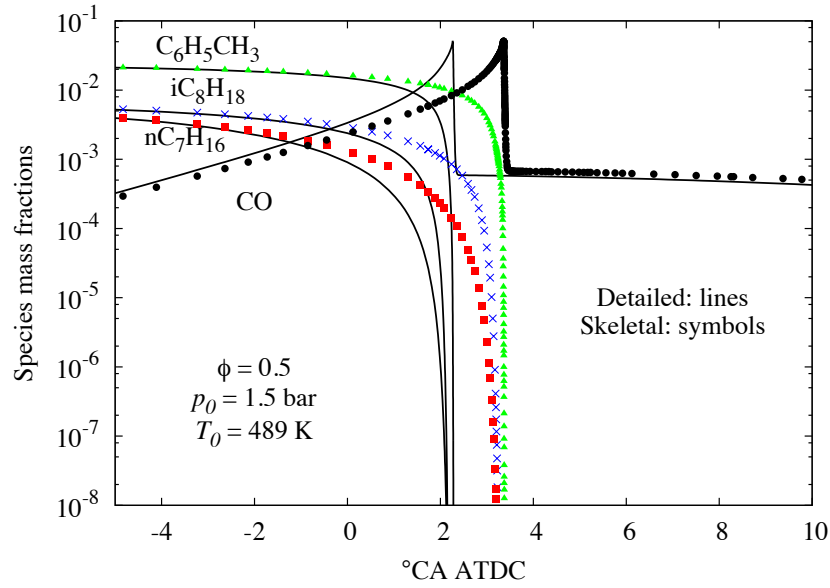


(a) Original CA

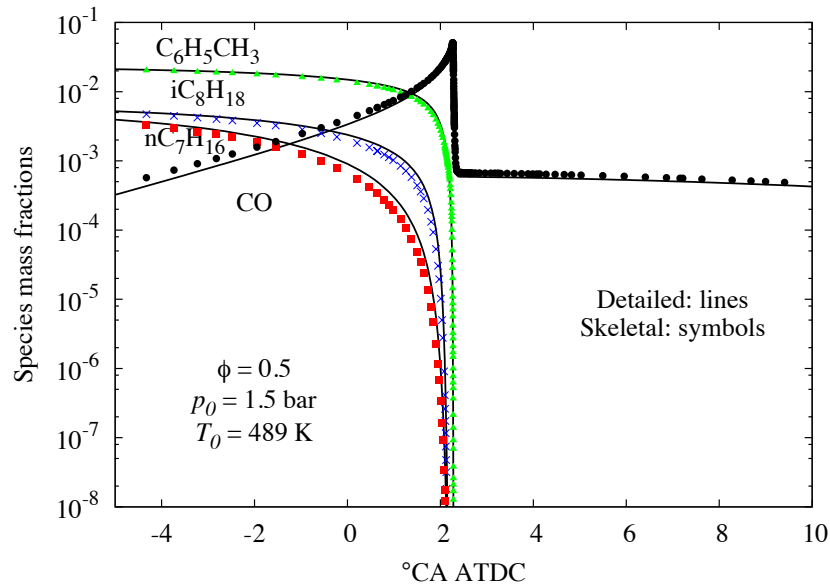


(b) Shifted CA

Figure S7: Comparison of major species mass fractions between the detailed TRF and 30%-error comprehensive skeletal (276 species and 936 reactions) mechanisms for a single-zone HCCI simulation with the IC3 initial conditions specified in Table 1. The shifted CA plot is based on ignition delay timing.

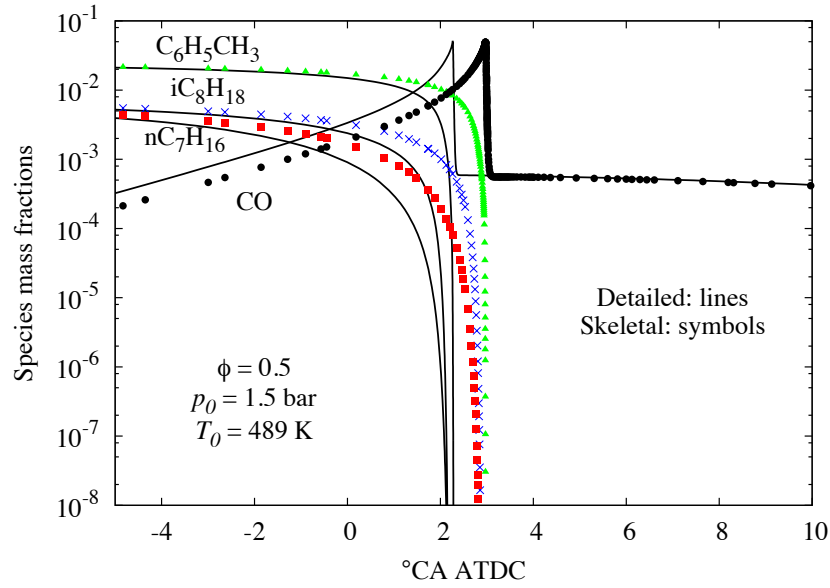


(a) Original CA

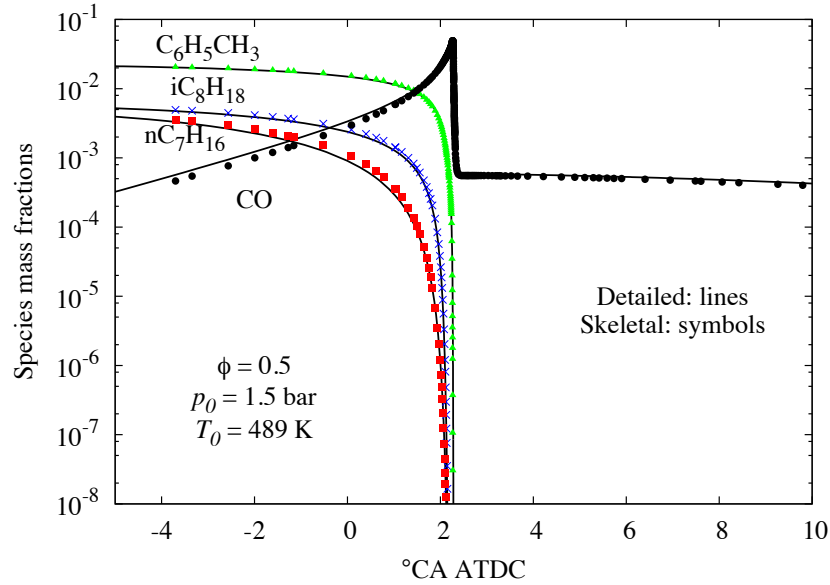


(b) Shifted CA

Figure S8: Comparison of major species mass fractions between the detailed TRF and 10%-error comprehensive skeletal (386 species and 1,591 reactions) mechanisms for a single-zone HCCI simulation with the IC4 initial conditions specified in Table 1. The shifted CA plot is based on ignition delay timing.



(a) Original CA



(b) Shifted CA

Figure S9: Comparison of major species mass fractions between the detailed TRF and 30%-error comprehensive skeletal (276 species and 936 reactions) mechanisms for a single-zone HCCI simulation with the IC4 initial conditions specified in Table 1. The shifted CA plot is based on ignition delay timing.